

Deep Learning for Motion Classification in Ankle Exoskeletons Using Surface EMG and IMU Signals

Silas Ruhrberg Estévez^{1,2}, Josée Mallah¹, Dominika Kazieczko¹, Chenyu Tang¹, and Luigi G. Occhipinti^{1,*}

¹Electrical Engineering Division, Department of Engineering, University of Cambridge, Cambridge CB3 0FA, UK

²School of Clinical Medicine, University of Cambridge, Cambridge CB2 0SP, UK

*lgo23@cam.ac.uk

Abstract

Ankle exoskeletons have garnered considerable interest for their potential to enhance mobility and reduce fall risks, particularly among the aging population. The efficacy of these devices relies on accurate real-time prediction of the user's intended movements through sensor-based inputs. This paper presents a novel motion prediction framework that integrates three Inertial Measurement Units (IMUs) and eight surface Electromyography (sEMG) sensors to capture both kinematic and muscular activity data. A comprehensive set of activities, representative of everyday movements in barrier-free environments, was recorded for the purpose. Our findings reveal that Convolutional Neural Networks (CNNs) slightly outperform Long Short-Term Memory (LSTM) networks on a dataset of five motion tasks, achieving classification accuracies of $96.5 \pm 0.8\%$ and $87.5 \pm 2.9\%$, respectively. Furthermore, we demonstrate the system's proficiency in transfer learning, enabling accurate motion classification for new subjects using just ten samples per class for finetuning. The robustness of the model is demonstrated by its resilience to sensor failures resulting in absent signals, maintaining reliable performance in real-world scenarios. These results underscore the potential of deep learning algorithms to enhance the functionality and safety of ankle exoskeletons, ultimately improving their usability in daily life.

Introduction

Globally, approximately one in ten people is over the age of 65, a proportion that is expected to double by the end of the century [1]. Among the elderly, an estimated 32% experience gait disturbances, which significantly increase their risk of falls [2]. In the United States and the United Kingdom, the annual cost of falls is estimated at \$50 billion [3] and \$2.6 billion [4], respectively. Ankle exoskeletons offer a promising solution to counteract the decline in muscle strength and balance associated with aging, potentially improving gait and reducing the risk of falls [5, 6]. Additionally, these devices may benefit a large group of patients suffering from conditions such as stroke, multiple sclerosis (MS), and cerebral palsy [7, 8, 9]. Healthy individuals may still benefit from exoskeleton during high effort manual labour tasks [10, 11, 12] and to reduce fatigue [13, 14].

Exoskeletons can be broadly categorized as either active or passive, based on the presence of an external power source [15]. Passive exoskeletons rely on mechanical components, such as springs, to assist walking by storing and releasing energy at specific points in the gait cycle [16]. In contrast, active exoskeletons incorporate actuators like electric motors or pneumatic systems to directly reduce the physical effort required for walking, and in some cases, enable walking without muscle activity [17, 18]. For optimal support of user movements, active exoskeletons must accurately classify the user's motion intentions and reduce the latency between sensor input and control system response [19]. To achieve this, a sensing system to record electrical activity, movements or forces must be designed. Common sensors used in lower limb applications include IMUs, surface EMGs, and force or pressure sensors [20].

The data from these sensors are processed, and motions classified using machine learning techniques including Support Vector Machines (SVM), Convolutional Neural Networks (CNN), and Long Short Term Memory Networks (LSTM). Although SVMs have achieved near-perfect classification accuracy, CNNs have not yet reached comparable levels of accuracy [20]. However, SVMs have limitations when it comes to training on large datasets or handling multi-class problems [21]. A study by Li *et al.* reported a classification accuracy of 95% using CNNs and LSTMs, but their work was limited to isolated ankle movements rather than activities of daily living[22]. Cheng *et al.* obtained similar results with a comparable approach [23]. In contrast, Kim *et al.* achieved an 88% accuracy in classifying motions of daily living activities using CNNs trained on EMG and IMU data, which, while promising, is still insufficient for a seamless user experience [24]. These studies highlight the potential of deep learning for motion classification, but do not achieve high enough accuracies to enable seamless user experiences.

This study aims to assess whether scalable models, such as LSTM or CNN, can achieve high accuracy when used with a non-invasive recording system. We will evaluate both IMU and surface EMG signals to determine their suitability for predicting ankle movements during activities of daily living. Electromyography (EMG) applications for long-term monitoring have traditionally been limited by the degradation of the skin-electrode interface, particularly when using conventional metal or gel electrodes. However, recent advancements in textile-based dry electrodes offer a promising alternative. These electrodes can be seamlessly integrated into clothing, providing enhanced comfort and durability for extended wear, while maintaining signal quality comparable to traditional methods [25]. Additionally, to demonstrate model generalizability, we will test the models' performance in transfer learning scenarios. For user safety, we will also assess how the models perform in the event of individual sensor failure during operation. Furthermore, we provide a new publicly available dataset of EMG and IMU data, along with the data processing code and machine learning models, to support the development of new classification methods for exoskeleton control.

Results

Data collection from human subjects

Ethical approval was obtained to record a total of 1,504 trials across three subjects using both EMG and IMU sensors (see Figure 1). IMU sensors were positioned on both shanks and on the right foot, while surface EMG sensors were placed to capture activity of the tibialis anterior, gastrocnemius medial and lateral heads, and soleus muscles. The five recorded motions, essential for navigating a barrier-free environment, included walking forwards, walking backwards, turning left, turning right, and squatting (to pick up an object or sit down). The collected signals were pre-processed and subsequently used to train a classifier for motion recognition.

Representative raw recordings from two different trials, illustrating expected behavior, are shown in Figure 2. During forward walking, the IMU's vertical acceleration exhibits several distinct peaks, corresponding to most steps. However, some steps lack clear peaks, likely due to the subject not lifting their feet significantly during those strides. Concurrently, the soleus muscle recordings show multiple activations, as expected, given its role in plantar flexion during forward propulsion [26]. In the squatting motion, activation of the tibialis anterior muscle is observed, which is essential for dorsiflexion to move the knees forwards [27]. This activation is followed by a noticeable increase in forward horizontal acceleration, capturing the movement pattern.

Motion classification using deep learning

For classification, both LSTM and CNN models were trained on IMU data, EMG data and the combined IMU and EMG data. Combining IMU and EMG data for both the CNN and LSTM models results in high performance (see Fig. 3). The CNN demonstrated a slight performance advantage over the LSTM, achieving an accuracy of $96.5 \pm 0.8\%$ on the test data, compared to the LSTM's $87.5 \pm 2.9\%$. As expected, models

trained on individual modalities, such as EMG or IMU data alone, showed lower but still acceptable classification accuracies. Specifically, CNNs trained on only EMG data reached $93.9 \pm 1.6\%$, while those trained on only IMU data achieved $93.3 \pm 1.6\%$. Additionally, given that some users may require exoskeleton support for only one leg, we evaluated the classification accuracy using EMG and IMU data from a single leg. In this case, the CNN achieved an accuracy of $92.9 \pm 1.6\%$, highlighting the robustness of the model even with reduced input channels.

A detailed performance analysis of the CNN on test data using all channels is shown using a confusion matrix (see Fig. 3) and precision, recall and F1 scores for the five classes (see Table 1). The CNN demonstrates high accuracy across all classes, with only minor confusion observed between certain motions. Specifically, slight misclassification occurs between Turn Left and Turn Right, as well as between Walking Forwards and Walking Backwards. This confusion is likely attributable to the engagement of similar muscle groups and the symmetrical nature of leg movements, despite the differences in direction.

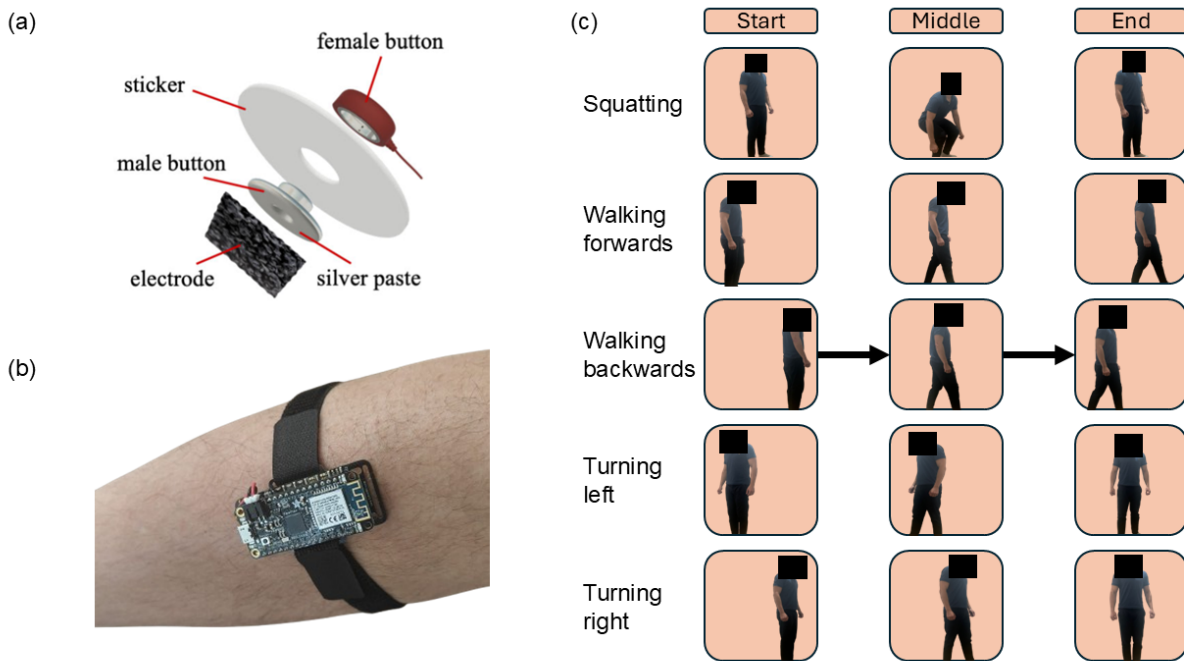


Figure 1: **Data collection** (a) The schematic illustrates the custom-made electrode assembly used for EMG recordings [25]. (b) Motion data was captured using commercial IMUs. (c) The dataset includes recordings from various activities: squatting, walking forwards and backwards, and turning left and right.

Motion	Precision	Recall	F1
Turn left	0.9757	0.9331	0.9539
Turn right	0.9483	0.9670	0.9576
Pick up object	0.9861	0.9658	0.9758
Backwards	0.9723	0.9565	0.9643
Forwards	0.9398	0.9969	0.9675

Table 1: **CNN performance metrics.**

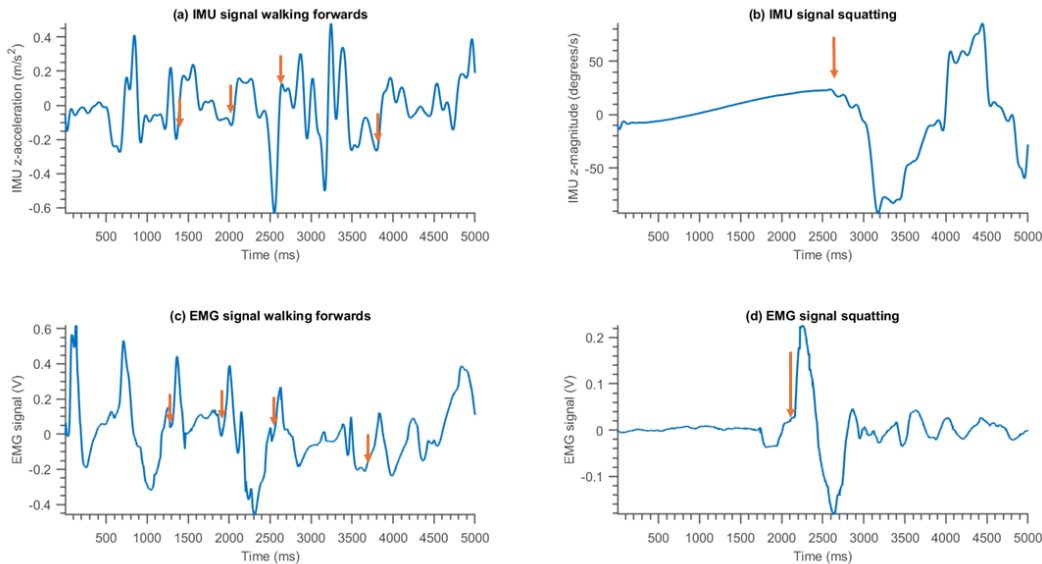


Figure 2: **Signal recordings** Representative examples of the relationship between recorded signals and physiological processes (a-d). During forward walking, intermittent forward acceleration is detected by the IMU (a), which corresponds to regular activation of the soleus muscle (c). Similarly, during a squat movement, slight forward motion of the shank is observed by the IMUs, which is linked to activity in the tibialis anterior muscle (d). Orange arrows highlight key instances where the two signals align, emphasizing representative matches. The EMG signal leads the IMU data, as there is an inherent latency between the electrical signals indicating muscle contraction and the subsequent initiation of motion detected by the IMU.

Transfer learning for model deployment

To demonstrate our model’s ability to generalize to new users, we trained the CNN on data from only two subjects and evaluated its performance on the third subject. As expected, the model’s accuracy was notably lower ($69.0 \pm 7.6\%$) (pretraining only) compared to the version trained on data from all three subjects ($96.5 \pm 0.8\%$) (original) (see Fig. 4). Additionally, training the model with only 10 samples per category from a new subject (finetuning only) resulted in very low accuracy of $58.0 \pm 6.7\%$. However, fine-tuning a pre-trained model using just 10 motion samples from the third subject achieved a performance of $89.7 \pm 3.7\%$. For this, the convolutional layers were frozen after the pre-training, while the fully connected layer could still be modified. Part of the small difference is likely due to the original model being trained on 1,204 samples, compared to 1,051 for the transfer learning model.

Model robustness to sensor failure during operation

During use, individual sensors may fail to provide accurate signals. For example, EMG electrodes might lose contact with the skin, or an IMU’s battery could deplete. In such cases, the model’s performance is likely to decrease due to the unexpected input from a faulty channel. However, it is crucial that the model maintains a sufficiently high level of performance to ensure the user’s safety, allowing them to notify caretakers and retain some mobility until the sensors can be replaced. To assess the model’s safety under these conditions, we evaluated classification accuracy on test samples where all channels of a particular sensor were set to zero, simulating absent signals, while the training samples remained unaltered. The model maintained an accuracy above 80% even when individual IMU sensors failed or when EMG signals from one leg were lost

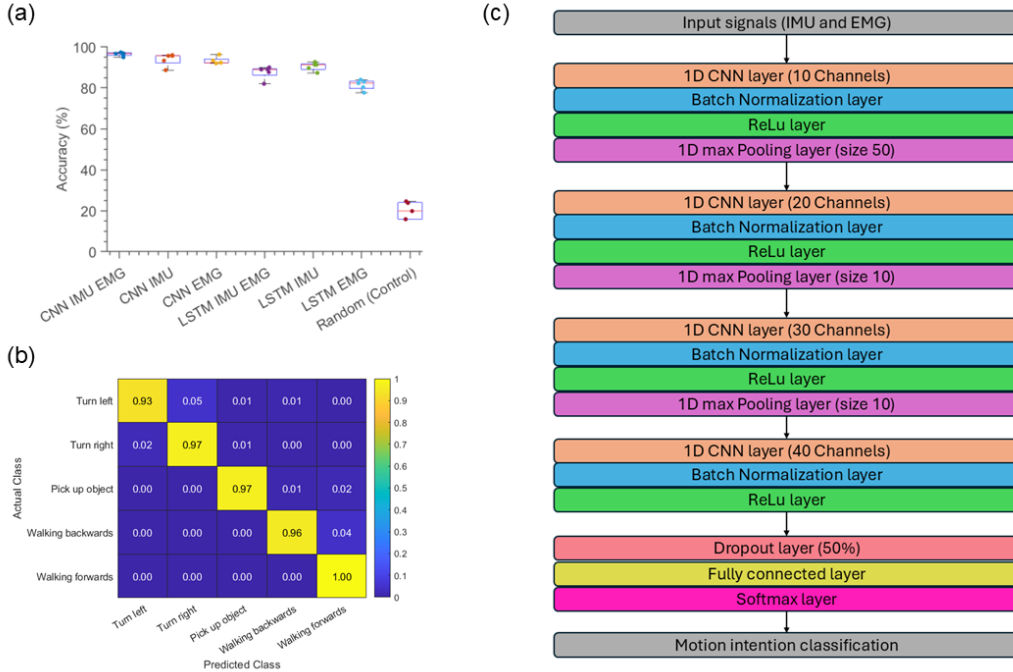


Figure 3: **Classifier performance** (a) Performance of LSTM and CNN trained on different datasets (IMU only, EMG only and combined EMG and IMU). As a control, the accuracy of randomly choosing a class for each test sample was also reported. (b) Confusion matrix for the CNN trained on both IMU and EMG data. (c) Architecture of the CNN used for motion classification.

(see Fig. 4). The most significant performance drop occurred when the IMU on the foot was deactivated, likely due to the limited availability of redundant signals. In this scenario, the classification accuracy fell to $82.8 \pm 2.9\%$, which is notably lower than the accuracies observed when the IMUs on the left and right shanks were deactivated, yielding $94.1 \pm 1.6\%$ and $95.7 \pm 0.8\%$, respectively. This suggests that the foot IMU plays a critical role in providing unique data for accurate classification.

Discussion

We demonstrate that EMG and IMU signals can be effectively utilized for high-accuracy motion intention prediction using a CNN. The proposed prototype is cost-efficient, built with commercially available IMU sensors and EMG electrodes, with minor modifications to the contact pads. Additionally, the machine learning models are lightweight, eliminating the need for external graphics cards during operation. Our model slightly outperforms comparable models for lower limb motion classification reported in the literature (see Table 2).

Study	Classes	Movements	Sensors	Model	Accuracy
Kim <i>et al.</i>	6	Full body	IMU + EMG	CNN	88.0%
Li <i>et al.</i>	6	Ankle only	EMG	CNN-LSTM	95.7%
Si <i>et al.</i>	5	Full body	EMG	CNN	95.5%
This work	5	Full body	IMU	CNN	93.3%
This work	5	Full body	EMG	CNN	93.9%
This work	5	Full body	IMU + EMG	CNN	96.5%

Table 2: Performance of similar machine learning models in the literature.

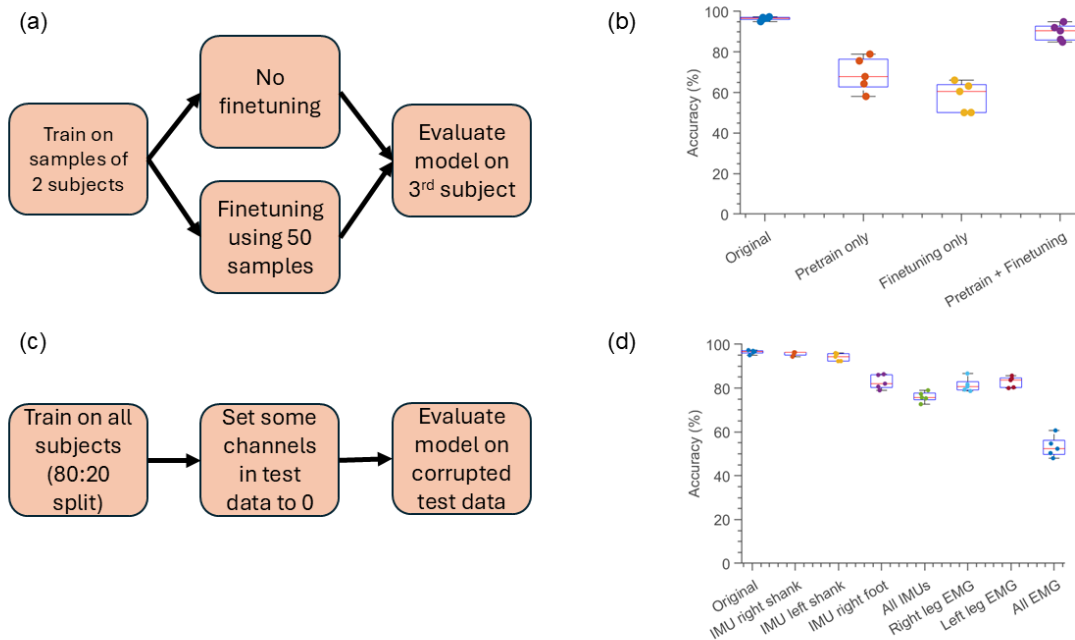


Figure 4: **Transfer learning and model robustness.** (a) For transfer learning the model is trained using data from 2 subjects only. The resulting model is then optionally fine-tuned using 50 samples before being evaluated on samples from a new subject. (b) Performance of the different models. (c) For model robustness the model is trained as previously but test data channels are corrupted. (d) The effect of different sensor corruptions on the classification results.

Importantly, unlike the work by Li *et al.*, our study involved full-body movements rather than limiting classification to isolated ankle motions, which are typically required for exoskeleton support [22]. This distinction makes direct comparisons challenging, as the movement classes we trained for are substantially different. The most comparable model in terms of sensor setup is that of Kim *et al.*, which also focused on motions needed for navigating an environment but achieved only 88% accuracy [24]. Additionally, the model by Si *et al.* achieved accuracy comparable to ours using only EMG recordings, but it focused on movements not commonly performed in daily life, such as a straight leg lift, which involve very different muscle activation patterns which likely facilitate classification [28].

The accuracy of our CNN trained solely on the EMG portion of the dataset is comparable to results reported in other studies (see Table 2). Notably, the model also demonstrated strong performance when trained using only the IMU data. This is particularly promising, as muscle atrophy in paralyzed patients can lead to altered or diminished EMG signals, making IMU data a valuable alternative [29]. These findings underscore that while each modality—EMG or IMU—can be effective for motion classification on its own, sensor fusion should be prioritized for more accurate and robust system development.

To the best of our knowledge, this is the first approach to incorporate textile electrodes in wearable exoskeleton control systems, which offer greater promise for long-term monitoring due to their comfort and wearability. Unlike previous studies, we specifically focused on evaluating model performance for motions that are most critical to exoskeleton operation. Furthermore, we conducted additional analyses to assess the feasibility of deploying our model in real-world settings, as well as its safety for users, ensuring that the system is both practical and secure for continuous use in assistive devices.

To effectively deploy an exoskeleton to new users, it is essential that the model generalizes well beyond

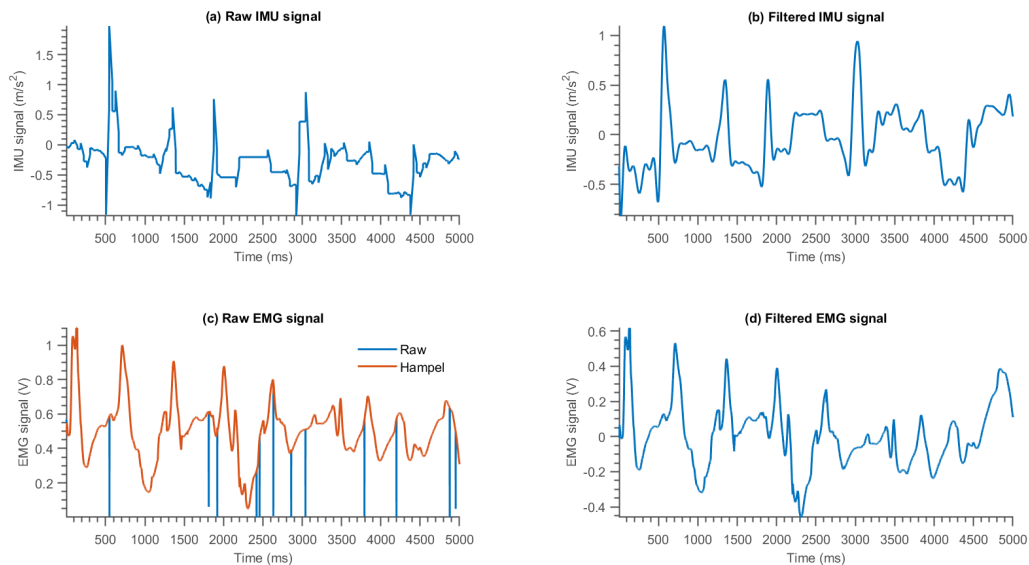


Figure 5: **Signal processing.** Representative examples of EMG and IMU signal processing recorded during a forward walking trial. (a) The raw IMU signals are bandpass filtered to reduce noise (b). (c) EMG signals undergo outlier removal using a Hampel filter before bandpass filtering (d).

the initial training dataset. Retraining the model for each individual would be both time-consuming and costly. However, previous studies have shown that fine-tuning with a small number of samples can still yield high-accuracy gesture classification [25, 30]. In our study, we trained the model on a minimal dataset of just two subjects and then used fine-tuning to generalize the model to a third subject. With minimal calibration, the system achieved high accuracy, suggesting that transfer learning is a viable approach for our model, enabling effective adaptation to new users with minimal data and effort.

Our model robustness testing indicates a high level of user safety in the event of unexpected sensor failure during operation. We evaluated extreme scenarios, including the complete failure of one or more sensors. Although model performance drops noticeably under these conditions, the accuracy remains sufficient for the system to capture the correct motion in real-time, albeit with some minor difficulties—such as needing to repeat movements until the model makes the correct inference. The performance drop could likely be mitigated further by augmenting the training data with examples of faulty channels. However, since it is impractical to anticipate every possible mode of sensor failure, we opted to use a zero-signal approach as a proof-of-concept example of an unencountered faulty signal. This demonstrates the model’s ability to handle sensor anomalies it was not explicitly trained on.

In conclusion, we present a robust system for accurate motion classification using surface EMG and IMU signals, with the highest accuracy achieved by a CNN that integrates both data modalities. The model shows strong generalizability to new users, requiring only minimal fine-tuning to maintain high performance. It also demonstrates resilience to individual sensor failures, continuing to deliver reliable accuracy even under suboptimal conditions. Furthermore, we validate the use of towel-based electrodes for motion intention applications, reinforcing the findings of Tang *et al.*, who demonstrated accurate digit classification of quasistatic movements such as hand gesture recognition using this innovative electrode system [25]. To support further research and development, we have made our code for data collection and analysis, as well as our datasets, publicly available—enabling the development of similar systems and machine learning models across the field.

The study has several limitations. First, we evaluated only a limited set of movements, which are adequate

for navigating barrier-free environments, but further testing should encompass more complex motions, such as stair ascent and descent. For comprehensive exoskeleton control, it will also be necessary to predict joint angles in addition to classifying movements, which will require the collection of additional ground-truth data. LSTM-CNN hybrid models have shown promising results in predicting joint angles and could be explored for this purpose [31]. Another limitation is that the system was tested on only three subjects, although the transfer learning results indicate good generalizability. Moreover, a fourth IMU on the left foot should ideally be added for a more comprehensive dataset. Additionally, the current setup requires the attachment of multiple EMG sensors, which can be time-consuming. This challenge could be addressed by integrating the textile electrodes into a comfortable, wearable leg sleeve, streamlining the setup process. Future research will focus on collecting larger, more diverse datasets, including joint angle measurements, and integrating the system into an exoskeleton to provide enhanced support for users in real-world environments.

Methods

EMG sensor fabrication

The conventional wet gel electrodes from a commercial three-electrode gel EMG setup (SeeedStudio EMG Detector) were replaced with custom-made textile electrodes, utilizing a graphene/PEDOT:PSS composite material [25]. The electrodes were fabricated using commercial cotton towels (NU249W, Aston Pharma), which were first cleaned by treatment with ethanol and UV/ozone. The cleaned towels were then soaked in a graphene solution for 30 minutes, followed by drying at 120°C for an additional 30 minutes. This process was repeated with an aqueous solution of PEDOT:PSS (ph1000, Ossila, diluted 1:10). The alternating cycles of soaking in graphene and PEDOT:PSS were repeated several times to create the final composite material.

Data collection

The EMG detector boards were connected to an ESP32-S3 microcontroller development board, which transmitted the data wirelessly over WiFi to a laptop. To measure motion, open-source commercially-available EmotiBit sensor units including 9-axis IMUs were employed [32]. The firmware for the IMU microcontrollers was manually developed using the manufacturer’s software [33] and the Espressif 32 functionality provided by PlatformIO. Data was wirelessly transmitted using the EmotiBit Oscilloscope Software, which streamed the data locally over a UDP stream. The dataset comprises five distinct classes of motion (Turn left (90°), Turn right (90°), Picking up an object from the floor, Walking forwards and Walking backwards), with each class containing approximately 100 samples per subject, ensuring equal distribution across the dataset.

Human subject study

Ethical approval for the study was granted by the University of Cambridge Department of Engineering Research Ethics Committee (registration number #394). All participants provided informed consent prior to the experiment. Data collection took place in the Human Performance Laboratory at the University of Cambridge. The study involved three young healthy volunteer participants (2 females, 1 male), with an average age of 23 ± 1 years, height 173 ± 9 cm, and weight 69 ± 16 kg. EMG data were collected bilaterally for tibialis anterior, gastrocnemius medial and lateral heads, and soleus muscles. The electrodes were placed according to the SENIAM guidelines [34]. The 3 IMU units were placed on the right and left shanks, and right foot.

Timestamp matching between modalities

The raw UDP stream from the EmotiBit oscilloscope was divided into three distinct files, each corresponding to data from a specific sensor. These files were processed using the EmotiBit DataParser, producing output files for the nine modalities associated with each IMU. The timestamps of the two recorded signals were then aligned to ensure synchronization. To match the frequency of the EMG signal, the IMU data were upsampled by a factor of 40 using linear interpolation. The final output for each trial was a CSV file, containing 35

columns and 5000 rows, representing a 5-second recording sampled at 1000 Hz.

Signal pre-processing

Signal processing was performed in MATLAB (version R2023b). The raw EMG values were converted to voltage V using the equation

$$V = \frac{1.1}{4095} \cdot S \quad (1)$$

where S are the raw signals and V is the output voltage in Volt, knowing that the on-board analog-to-digital converter (ADC) featured a 12-bit resolution and a reference voltage of 1.1 V. The signals were then passed through a Hampel filter that removed outliers deviating by more than three standard deviations from the 50 surrounding samples (see Fig. 5) [35]. The signals were then bandpass filtered using a fifth order Butterworth filter with cutoff frequencies of 0.2 and 400 Hz [36]. The signals were then normalised to zero mean and unit variance. Similarly, the raw IMU signals were bandpass filtered using a fifth-order Butterworth filter, but with cutoff frequencies of 0.2 Hz and 10 Hz, chosen based on the anticipated duration of the movements performed during the trial. These IMU signals were then normalized following the same procedure as the EMG signals.

Machine learning models

All models were trained using the MATLAB Deep Learning Toolbox (version 23.2). The dataset, consisting of recordings and labels, was randomly split into training (80%) and testing (20%) sets. The CNN architecture was adapted from a motion classification model by Tang *et al.* [25], and comprises several stages of 1D convolutional layers, each followed by batch normalization, ReLU activation, and max-pooling layers. These are followed by dropout layers, fully connected layers, and a softmax layer for classification. A detailed schematic of the CNN architecture is shown in Figure 3, while the model parameters are outlined in Table 3. The LSTM model was built using two LSTM layers, each containing 100 units, followed by a 20% dropout layer, a fully connected layer, and a softmax layer. This network structure is based on the two-layer LSTM example provided in the MATLAB documentation [37].

Both models were trained using cross-entropy loss and optimized with the ADAM optimizer, using a batch size of 50 over 15 epochs. Performance metrics included accuracy, precision, recall, and F1 score. Training was conducted on the CPU of a Dell XPS 13 laptop (Intel i7), with individual CNN training times not exceeding 5 minutes. Each model was trained using five different random seeds, and performance metrics were averaged across these runs.

Statistical analysis

Model performance was evaluated using accuracy, precision, recall, and F1 scores, as outlined in Hicks *et al.* [38]. Accuracy, the most straightforward metric, represents the fraction of correctly classified samples and is calculated as:

$$\text{Accuracy} = \frac{TC}{TC + FC} \quad (2)$$

where TC is the number of true classifications, and FC represents false classifications across all samples. This metric is particularly suitable for our evaluation because our dataset is balanced, ensuring that accuracy provides a meaningful overall assessment.

Precision measures how many of the samples predicted to belong to a particular class actually do, and is given by:

$$\text{Precision} = \frac{TP}{TP + FP} \quad (3)$$

Layer (type)	Output shape	Parameter number
Cov-1D-1	[50, 10, 5000]	3160
BatchNorm	[50, 10, 5000]	20
MaxPool1D	[50, 10, 100]	0
Cov-1D-2	[50, 20, 100]	1820
BatchNorm	[50, 20, 100]	40
MaxPool1D	[50, 20, 10]	0
Cov-1D-3	[50, 30, 10]	5430
BatchNorm	[50, 30, 10]	60
MaxPool1D	[50, 30, 1]	0
Cov-1D-1	[50, 40, 1]	10840
BatchNorm	[50, 40, 1]	80
Dropout	[50, 40, 1]	0
FullyConnected	[50, 5]	205
Total parameters	-	21655
Trainable parameters	-	21655
Non-trainable parameters	-	0

Table 3: Calculation of parameters in the CNN. The output shape is given as [batch size, number of channels, channel length].

Here, TP represents true positives, and FP denotes false positives for a specific class. Precision is useful in cases where minimizing false positives is critical.

Recall, on the other hand, quantifies the proportion of actual class members that were correctly identified, and is defined as:

$$\text{Recall} = \frac{TP}{TP + FN} \quad (4)$$

In this case, FN refers to false negatives, or instances where the model failed to identify the true class. Recall is valuable when minimizing false negatives is a priority.

Finally, the F1 score combines precision and recall into a single metric that balances both, particularly useful when there is an uneven trade-off between the two. The F1 score is calculated as:

$$\text{F1} = \frac{2 \cdot \text{Precision} \cdot \text{Recall}}{\text{Precision} + \text{Recall}} \quad (5)$$

This harmonic mean provides a robust measure when dealing with imbalanced class distributions or when both precision and recall are equally important in evaluating model performance.

References

- [1] Danan Gu, Kirill Andreev, and Matthew E. Dupre. Major trends in population growth around the world. *China CDC Weekly*, 3(28):604–613, 2021. ISSN 2096-7071. doi: 10.46234/ccdcw2021.160. URL <http://dx.doi.org/10.46234/ccdcw2021.160>.
- [2] Philipp Mahlknecht, Stefan Kiechl, Bastiaan R. Bloem, Johann Willeit, Christoph Scherfler, Arno Gasperi, Gregorio Rungger, Werner Poewe, and Klaus Seppi. Prevalence and burden of gait disorders in elderly men and women aged 60–97 years: A population-based study. *PLoS ONE*, 8(7):e69627, July 2013. ISSN 1932-6203. doi: 10.1371/journal.pone.0069627. URL <http://dx.doi.org/10.1371/journal.pone.0069627>.
- [3] Curtis S. Florence, Gwen Bergen, Adam Atherly, Elizabeth Burns, Judy Stevens, and Cynthia Drake. Medical costs of fatal and nonfatal falls in older adults. *Journal of the American Geriatrics Society*, 66(4):693–698, March 2018. ISSN 1532-5415. doi: 10.1111/jgs.15304. URL <http://dx.doi.org/10.1111/jgs.15304>.

- [4] The human cost of falls 2013; UK Health Security Agency — ukhsa.blog.gov.uk. <https://ukhsa.blog.gov.uk/2014/07/17/the-human-cost-of-falls/>. [Accessed 24-10-2024].
- [5] Martin Grimmer, Robert Riener, Conor James Walsh, and André Seyfarth. Mobility related physical and functional losses due to aging and disease - a motivation for lower limb exoskeletons. *Journal of NeuroEngineering and Rehabilitation*, 16(1), January 2019. ISSN 1743-0003. doi: 10.1186/s12984-018-0458-8. URL <http://dx.doi.org/10.1186/s12984-018-0458-8>.
- [6] Michael Raitor, Sandra Waugh Ruggles, Scott L. Delp, C. Karen Liu, and Steven H. Collins. Lower-limb exoskeletons appeal to both clinicians and older adults, especially for fall prevention and joint pain reduction. *IEEE Transactions on Neural Systems and Rehabilitation Engineering*, 32:1577–1585, 2024. doi: 10.1109/TNSRE.2024.3381979.
- [7] Bin Shi, Xiaofeng Chen, Zan Yue, Shuai Yin, Qipeng Weng, Xue Zhang, Jing Wang, and Weina Wen. Wearable ankle robots in post-stroke rehabilitation of gait: A systematic review. *Frontiers in Neurorobotics*, 13, August 2019. ISSN 1662-5218. doi: 10.3389/fnbot.2019.00063. URL <http://dx.doi.org/10.3389/fnbot.2019.00063>.
- [8] Ghaith J. Androwis, Brian M. Sandroff, Peter Niewrzol, Farris Fakhoury, Glenn R. Wylie, Guang Yue, and John DeLuca. A pilot randomized controlled trial of robotic exoskeleton-assisted exercise rehabilitation in multiple sclerosis. *Multiple Sclerosis and Related Disorders*, 51:102936, June 2021. ISSN 2211-0348. doi: 10.1016/j.msard.2021.102936. URL <http://dx.doi.org/10.1016/j.msard.2021.102936>.
- [9] Markus Hunt, Laure Everaert, Mathew Brown, Luiza Muraru, Eleni Hatzidimitriadou, and Kaat Desloovere. Effectiveness of robotic exoskeletons for improving gait in children with cerebral palsy: A systematic review. *Gait & Posture*, 98:343–354, October 2022. ISSN 0966-6362. doi: 10.1016/j.gaitpost.2022.09.082. URL <http://dx.doi.org/10.1016/j.gaitpost.2022.09.082>.
- [10] Yong K. Cho, Kinam Kim, Shaojun Ma, and Jun Ueda. A robotic wearable exoskeleton for construction worker’s safety and health. In *Construction Research Congress 2018*, volume 2013, page 19–28. American Society of Civil Engineers, March 2018. doi: 10.1061/9780784481288.003. URL <http://dx.doi.org/10.1061/9780784481288.003>.
- [11] Zefeng Yan, Bin Han, Zihao Du, Tiantian Huang, Ou Bai, and Ansi Peng. Development and testing of a wearable passive lower-limb support exoskeleton to support industrial workers. *Biocybernetics and Biomedical Engineering*, 41(1):221–238, January 2021. ISSN 0208-5216. doi: 10.1016/j.bbe.2020.12.010. URL <http://dx.doi.org/10.1016/j.bbe.2020.12.010>.
- [12] Fatai Sado, Hwa Jen Yap, Raja Ariffin Raja Ghazilla, and Norhafizan Ahmad. Design and control of a wearable lower-body exoskeleton for squatting and walking assistance in manual handling works. *Mechatronics*, 63:102272, November 2019. ISSN 0957-4158. doi: 10.1016/j.mechatronics.2019.102272. URL <http://dx.doi.org/10.1016/j.mechatronics.2019.102272>.
- [13] Zhuo Wang, Xinyu Wu, Yu Zhang, Chunjie Chen, Shoubin Liu, Yida Liu, Ansi Peng, and Yue Ma. A semi-active exoskeleton based on emgs reduces muscle fatigue when squatting. *Frontiers in Neurorobotics*, 15, April 2021. ISSN 1662-5218. doi: 10.3389/fnbot.2021.625479. URL <http://dx.doi.org/10.3389/fnbot.2021.625479>.
- [14] Wei Wei, Shijia Zha, Yuxuan Xia, Jihua Gu, and Xichuan Lin. A hip active assisted exoskeleton that assists the semi-squat lifting. *Applied Sciences*, 10(7):2424, April 2020. ISSN 2076-3417. doi: 10.3390/app10072424. URL <http://dx.doi.org/10.3390/app10072424>.
- [15] Monica Tiboni, Alberto Borboni, Fabien Vêrité, Chiara Bregoli, and Cinzia Amici. Sensors and actuation technologies in exoskeletons: A review. *Sensors*, 22(3):884, January 2022. ISSN 1424-8220. doi: 10.3390/s22030884. URL <http://dx.doi.org/10.3390/s22030884>.
- [16] Ettore Etenzi, Riccardo Borzuola, and Alena M. Grabowski. Passive-elastic knee-ankle exoskeleton reduces the metabolic cost of walking. *Journal of NeuroEngineering and Rehabilitation*, 17(1), July 2020. ISSN 1743-0003. doi: 10.1186/s12984-020-00719-w. URL <http://dx.doi.org/10.1186/s12984-020-00719-w>.

- [17] Patrick Slade, Mykel J. Kochenderfer, Scott L. Delp, and Steven H. Collins. Personalizing exoskeleton assistance while walking in the real world. *Nature*, 610(7931):277–282, October 2022. ISSN 1476-4687. doi: 10.1038/s41586-022-05191-1. URL <http://dx.doi.org/10.1038/s41586-022-05191-1>.
- [18] Bing Chen, Chun-Hao Zhong, Xuan Zhao, Hao Ma, Xiao Guan, Xi Li, Feng-Yan Liang, Jack Chun Yiu Cheng, Ling Qin, Sheung-Wai Law, and Wei-Hsin Liao. A wearable exoskeleton suit for motion assistance to paralysed patients. *Journal of Orthopaedic Translation*, 11:7–18, October 2017. ISSN 2214-031X. doi: 10.1016/j.jot.2017.02.007. URL <http://dx.doi.org/10.1016/j.jot.2017.02.007>.
- [19] Chenyu Tang, Zhenyu Xu, Edoardo Occhipinti, Wentian Yi, Muzi Xu, Sanjeev Kumar, Gurvinder S. Virk, Shuo Gao, and Luigi G. Occhipinti. From brain to movement: Wearables-based motion intention prediction across the human nervous system. *Nano Energy*, 115:108712, October 2023. ISSN 2211-2855. doi: 10.1016/j.nanoen.2023.108712. URL <http://dx.doi.org/10.1016/j.nanoen.2023.108712>.
- [20] Duojin Wang, Xiaoping Gu, and Hongliu Yu. Sensors and algorithms for locomotion intention detection of lower limb exoskeletons. *Medical Engineering & Physics*, 113:103960, March 2023. ISSN 1350-4533. doi: 10.1016/j.medengphy.2023.103960. URL <http://dx.doi.org/10.1016/j.medengphy.2023.103960>.
- [21] Jair Cervantes, Farid Garcia-Lamont, Lisbeth Rodríguez-Mazahua, and Asdrubal Lopez. A comprehensive survey on support vector machine classification: Applications, challenges and trends. *Neurocomputing*, 408:189–215, September 2020. ISSN 0925-2312. doi: 10.1016/j.neucom.2019.10.118. URL <http://dx.doi.org/10.1016/j.neucom.2019.10.118>.
- [22] Min Li, Jiale Wang, Shiqi Yang, Jun Xie, Guanghua Xu, and Shan Luo. A cnn-lstm model for six human ankle movements classification on different loads. *Frontiers in Human Neuroscience*, 17, March 2023. ISSN 1662-5161. doi: 10.3389/fnhum.2023.1101938. URL <http://dx.doi.org/10.3389/fnhum.2023.1101938>.
- [23] Hao-Ran Cheng, Guang-Zhong Cao, Cai-Hong Li, Aibin Zhu, and Xiaodong Zhang. A cnn-lstm hybrid model for ankle joint motion recognition method based on semg. In *2020 17th International Conference on Ubiquitous Robots (UR)*, pages 339–344, 2020. doi: 10.1109/UR49135.2020.9144698.
- [24] Jihoon Kim, Prakyath Kantharaju, Hoon Yi, Michael Jacobson, Hyungkeun Jeong, Hojoong Kim, Jinwoo Lee, Jared Matthews, Nathan Zavanelli, Hyeonseok Kim, Heejin Jeong, Myunghye Kim, and Woon-Hong Yeo. Soft wearable flexible bioelectronics integrated with an ankle-foot exoskeleton for estimation of metabolic costs and physical effort. *npj Flexible Electronics*, 7(1), January 2023. ISSN 2397-4621. doi: 10.1038/s41528-023-00239-2. URL <http://dx.doi.org/10.1038/s41528-023-00239-2>.
- [25] Chenyu Tang, Wentian Yi, Sanjeev Kumar, Gurvinder Singh Virk, and Luigi G. Occhipinti. Emg-based human motion analysis: A novel approach using towel electrodes and transfer learning. *IEEE Sensors Journal*, 24(6):9115–9123, 2024. doi: 10.1109/JSEN.2024.3354307.
- [26] Adrian Lai, Glen A. Lichtwark, Anthony G. Schache, Yi-Chung Lin, Nicholas A. T. Brown, and Marcus G. Pandy. In vivo behavior of the human soleus muscle with increasing walking and running speeds. *Journal of Applied Physiology*, 118(10):1266–1275, May 2015. ISSN 1522-1601. doi: 10.1152/jappphysiol.00128.2015. URL <http://dx.doi.org/10.1152/jappphysiol.00128.2015>.
- [27] Yong-wook Kim, Tea-heon Kim, Mi-na Yang, Ye-seul Yon, and Ji-hye Lee. Comparison of activities of tibialis anterior, peroneus longus, and tibialis posterior muscles according to lunge squats and bulgarian split squats in a healthy population. *Journal of KEMA*, 1(1):26–30, December 2017. ISSN 2586-4351. doi: 10.29273/jkema.2017.1.1.26. URL <http://dx.doi.org/10.29273/jkema.2017.1.1.26>.
- [28] Xiayi Si, Yuehong Dai, and Junyao Wang. Recognition of lower limb movements baesd on electromyography (emg) texture maps. In *2022 IEEE 5th International Conference on Electronics Technology (ICET)*, pages 1091–1095, 2022. doi: 10.1109/ICET55676.2022.9824410.

- [29] Chengjun Huang, Maoqi Chen, Yingchun Zhang, Sheng Li, and Ping Zhou. Model-based analysis of muscle strength and emg-force relation with respect to different patterns of motor unit loss. *Neural Plasticity*, 2021:1–9, June 2021. ISSN 2090-5904. doi: 10.1155/2021/5513224. URL <http://dx.doi.org/10.1155/2021/5513224>.
- [30] Ulysse Cote-Allard, Cheikh Latyr Fall, Alexandre Drouin, Alexandre Campeau-Lecours, Clement Gosselin, Kyrre Glette, Francois Laviolette, and Benoit Gosselin. Deep learning for electromyographic hand gesture signal classification using transfer learning. *IEEE Transactions on Neural Systems and Rehabilitation Engineering*, 27(4):760–771, April 2019. ISSN 1558-0210. doi: 10.1109/tnsre.2019.2896269. URL <http://dx.doi.org/10.1109/TNSRE.2019.2896269>.
- [31] Meng Zhu, Xiaorong Guan, Zhong Li, Long He, Zheng Wang, and Keshu Cai. semg-based lower limb motion prediction using cnn-lstm with improved pca optimization algorithm. *Journal of Bionic Engineering*, 20(2):612–627, October 2022. ISSN 2543-2141. doi: 10.1007/s42235-022-00280-3. URL <http://dx.doi.org/10.1007/s42235-022-00280-3>.
- [32] EmotiBit. EmotiBit.com — emotibit.com. <https://www.emotibit.com/>. [Accessed 26-08-2024].
- [33] Releases · EmotiBit/ofxEmotiBit — github.com. <https://github.com/EmotiBit/ofxEmotiBit/releases>. [Accessed 24-10-2024].
- [34] Recommendations for sensor locations in lower leg or foot muscles — seniam.org. http://seniam.org/lowerleg_location.htm. [Accessed 24-10-2024].
- [35] Susmit Bhowmik, Beth Jelfs, Sridhar P. Arjunan, and Dinesh K. Kumar. Outlier removal in facial surface electromyography through hampel filtering technique. In *2017 IEEE Life Sciences Conference (LSC)*, pages 258–261, 2017. doi: 10.1109/LSC.2017.8268192.
- [36] Carlo J. De Luca, L. Donald Gilmore, Mikhail Kuznetsov, and Serge H. Roy. Filtering the surface emg signal: Movement artifact and baseline noise contamination. *Journal of Biomechanics*, 43(8):1573–1579, May 2010. ISSN 0021-9290. doi: 10.1016/j.jbiomech.2010.01.027. URL <http://dx.doi.org/10.1016/j.jbiomech.2010.01.027>.
- [37] Long short-term memory neural networks. <https://uk.mathworks.com/help/deeplearning/ug/long-short-term-memory-networks.html>. [Accessed 24-10-2024].
- [38] Steven A. Hicks, Inga Strümke, Vajira Thambawita, Malek Hammou, Michael A. Riegler, Pål Halvorsen, and Sravanthi Parasa. On evaluation metrics for medical applications of artificial intelligence. *Scientific Reports*, 12(1), April 2022. ISSN 2045-2322. doi: 10.1038/s41598-022-09954-8. URL <http://dx.doi.org/10.1038/s41598-022-09954-8>.

Code availability

The underlying code for this study is available on GitHub and can be accessed via this link <https://github.com/Sr933/Exoskeleton-Data-Acquisition-and-Processing-Code>.

Data availability

The datasets generated and/or analysed during the current study are available in the Apollo repository and can be accessed via this link <https://doi.org/10.17863/CAM.113504>.

Acknowledgements

This study was partially funded by The MathWorks, Inc. The funder played no role in study design, data collection, analysis and interpretation of data, or the writing of this manuscript.

Author contributions statement

L.O. and J.M came up with the idea for the project. S.R.E, J.M. and D.K. designed the sensor system and collected the datasets. S.R.E. and C.T. performed the data analysis and designed the ML models. S.R.E drafted the first version of the manuscript. L.O. provided the overall guidance and resources for the project. All authors reviewed the manuscript.

Competing interests

The authors declare no competing interests.